

# Multi-Sensor Data Fusion for Seafloor Mapping and Ordnance Location

John Wright, Ken Scott, Tien-Hsin Chao, and Brian Lau

john.r.wright@jpl.nasa.gov

Jet Propulsion Laboratory

California Institute of Technology

4800 Oak Grove Drive

Pasadena, California 91109

under contract with National Aeronautics and Space Administration

John Lathrop and John McCormick

NAVSURFWARCEN COASTSYSTA

DAHLGREN DIV

**Abstract** – Results of ongoing work in developing methods for performing multi-sensor fusion for the purpose of locating unexploded ordnance in shallow water and creating models of the seafloor for visualization are presented. The sensor suite includes a forward-looking sonar, a low frequency side-looking sonar, a high frequency side-looking sonar, a magnetic field gradiometer, and an electro-optic laser-scanning sensor. Data fusion techniques discussed include an iterative method of performing automatic target recognition processing (ATRP) on individual sensor channels, correlating the individual sensor channels for a single pass using the target locations to assist the process, performing correlations on multiple passes over the same target area, and returning the correlated data to the ATRP algorithms. The second pass of the ATRP algorithms on the correlated data provides an additional method for locating and identifying targets while rejecting clutter. The focus is on the multi-sensor correlation and fusion techniques rather than the ATRP algorithms. Correlated sensor data, along with GPS information, is used to create three-dimensional models of the sea floor. The sea-floor models are used for visualization of the area around an item of unexploded ordnance to assist in planning remediation of the site. Fusion of multi-sensor data, and the production of models of the sea floor, are important capabilities for autonomous underwater vehicles. The models can be used for autonomous vehicle navigation and operation while the data may be transmitted to a base station for additional analysis purposes.

**Keywords:** Underwater vehicles, multi-sensor fusion, data mining, data visualization.

## Introduction

The Mobile Underwater Debris Survey System, or MUDSS, project seeks to develop a system to assist in cleaning up unexploded ordnance from shallow water areas. A number of areas around the United States have been used as test and practice ranges by our armed forces. These Formerly Used Defense Sites (FUDS) include Kahoolawe in Hawaii,

Amaknak and Adak in Alaska, and several sites along the east and gulf coasts. The MUDSS system is designed to assist in locating, classifying, and identifying the different ordnance within a survey area. These can range from 60 mm mortar shells up to 2000 pound bombs.

The MUDSS system is being developed in a joint effort between the Navy's Coastal Systems Station (CSS) and NASA's Jet Propulsion Laboratory (JPL) under the auspices of SERDP, the Strategic Environmental Research and Development Program. Phase I of the project, the Feasibility Demonstration, leverages technology developed for mine hunting into a prototype demonstration system. The system contains several sensors which scan the seafloor. Multisensor fusion techniques, leveraged from JPL's image processing and visualization work, combine the data from the various sensors to extract the maximum amount of information for locating and identifying the ordnance. In addition, topographic models of the seafloor may be developed which can aid in navigation and remediation activities.

Lessons learned from the MUDSS project may be applicable to the operation of Autonomous Underwater Vehicles (AUV). This paper describes the results of ongoing analysis of the sensor data collected during the Feasibility Demonstration tests and discusses future development of the system.

## System Description

The Feasibility Demonstration system uses sensors mounted on two pods suspended below a 40 foot catamaran (Figure 1). The front pod, a deadweight depressor, contains a forward-looking sonar, a high frequency side-looking sonar, and an electro-optic laser scanning sensor. The back pod, the towfish, is neutrally buoyant and is towed 17 meters behind the depressor. The towfish contains a low frequency side-looking sonar and a superconducting magnetic field gradiometer. The data from the sensors is transmitted via cable to the electronics shack on the catamaran containing the data processing, storage, and computing systems. A GPS system is used, in differential mode, to record the boat position during data acquisition passes. The catamaran

provides a stable platform for the mechanical assemblies and the shack housing the computing equipment. Two outboard motors are used to drive the catamaran at the desired speed of 3 knots. A winch assembly with shock absorbers buffers the depressor from the action of waves and wakes on the catamaran.

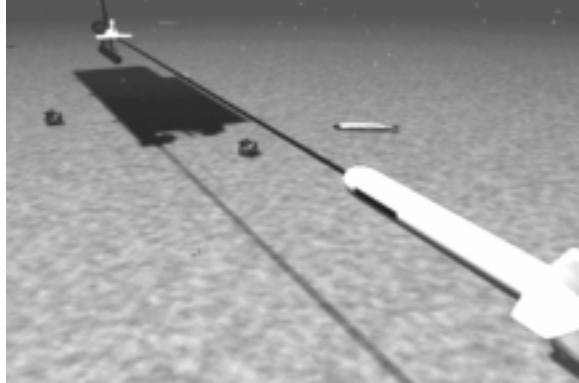


Figure 1 - Depressor and Towfish

The low frequency side-looking sonar is the primary sensor used for detecting ordnance. Its bottom penetrating capability and good resolution produce excellent images for detecting the entire range of expected ordnance. The high frequency side-looking sonar does not penetrate the bottom but produces high-resolution images of proud targets with shadows. The magnetic field gradiometer detects smaller ferrous targets near the sensor and large targets farther away, even when buried. The forward-looking sonar is a long range sensor for detecting proud targets which can also be used for target reacquisition. The electro-optic sensor produces high-resolution images of a narrow swath directly beneath the depressor. These images can be used to make the final identification of a suspected ordnance.

### Test Conditions

The Feasibility Demonstration tests were conducted in St. Andrew's Bay, Florida, near CSS. The water averaged 10 meters in depth with a nearly flat bottom of silt and sand. A clumped field of inert ordnance was laid down by divers in two concentric circles and the positions of the larger ordnance located with GPS. Six items of smaller ordnance were placed in an inner circle with a radius of 3 meters while four items of larger ordnance and two steel drums were placed on an outer circle with a radius of 11 meters. In addition, several panels with regular markings were laid down within the inner circle to test the resolution of the electro-optic sensor.

The depressor was lowered until it was approximately 5 meters above the seafloor. Multiple sensor runs were conducted by traversing past the clumped field at various angles and distances.

A second field, the linear field, was laid down with the ordnance positioned farther apart along a straight line. This field was used to test the gradiometer which cannot

distinguish multiple ordnance close together as in the clumped field. Again the positions of the ordnance were measured using GPS. Multiple sensor runs were conducted by traversing parallel to the field at various distances.

### Sensor Characteristics

The side-looking sonars are used in a synthetic aperture mode by performing beamforming as a postprocess on the collected data. The low frequency sonar has a range of 37 meters and a range resolution of 7.5 cm which is reduced to about 11 cm in the beamforming operation. The sonar can detect targets buried in a soft bottom up to 2 meters below the surface. An example of the low frequency sonar data appears in Figure 2. This is a view of the clumped target test field. Note the two concentric circles of target returns and the echoes from the larger returns due to multipathing. The low frequency sonar also gets a bottom return which can be used to estimate the depth of the water column beneath the sonar along the path of the towfish.

The high frequency side-looking sonar also has a range of 37 meters but has a range resolution of 5 cm. The beamforming operation reduces the range resolution to about 11 cm to match the low frequency sonar imagery. The high frequency sonar does not penetrate the bottom significantly and does not refract around objects so proud targets cast a shadow. An example of the high frequency sonar data appears in Figure 3. This view is also of the clumped test field from the same aspect as the low frequency view in Figure 2. Note the

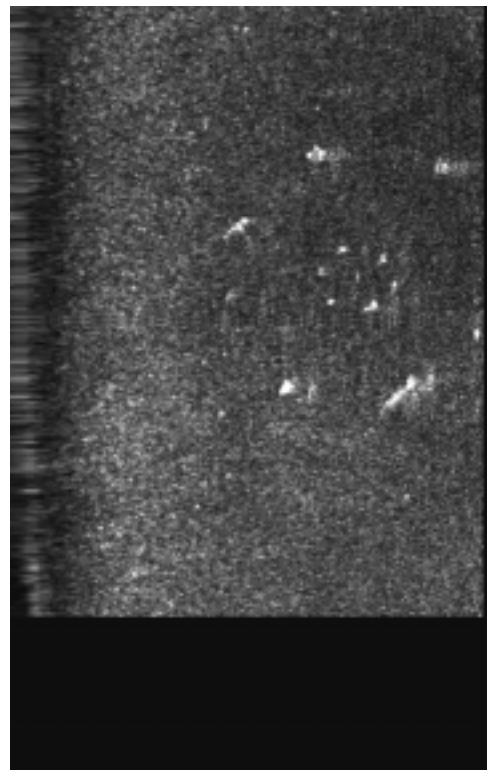


Figure 2 - Low Frequency Sonar Data

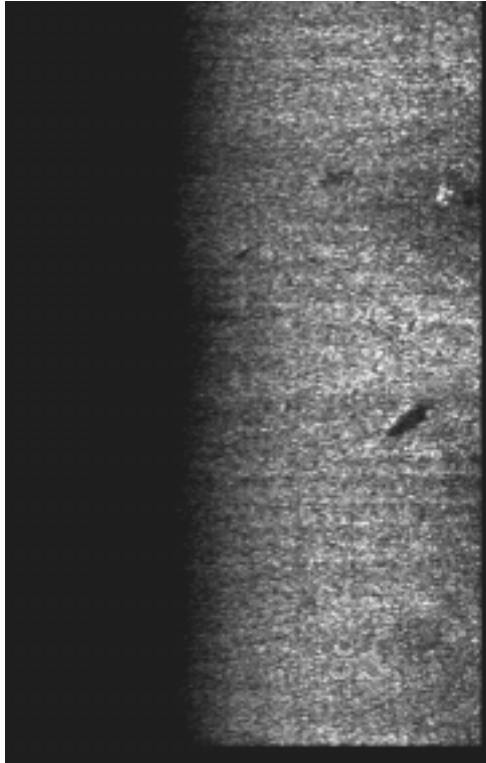


Figure 3 - High Frequency Sonar Data

definite shadows and the relative absence of echoes.

The superconducting magnetic field gradiometer senses variations in the earth's magnetic field due to the presence of ferrous metals. It can detect smaller ordnance at a range of five meters and larger ordnance out to 50 meters. It determines the position and magnetic moment of the ferrous objects within its range and can detect even deeply buried ordnance. The catamaran and the sensor pods are constructed of fiberglass, while the engines are aluminum, to minimize their effect on the operation of the gradiometer. The gradiometer produces a stream of moment and gradient data which must be postprocessed to produce a set of target locations relative to the gradiometer path.

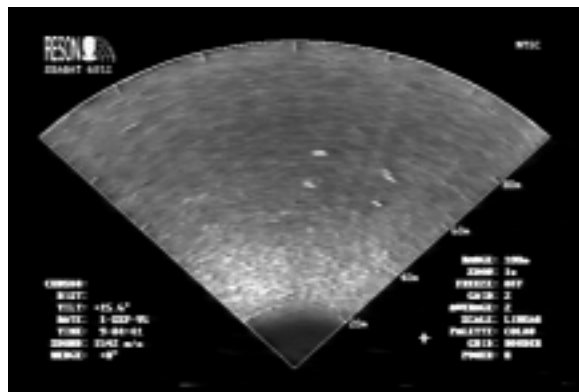


Figure 4 - Forward-Looking Sonar Data

The forward-looking sonar has a 90 degree field of regard, divided into 1.5 degree increments, with a maximum range of 200 meters and a range resolution of five cm. It has a digital and a video output but for the Feasibility Demonstration only the video output was used, thus reducing the effective range resolution to about 50 cm. The sonar does not significantly penetrate the bottom so its use is limited to detecting proud targets. An example of the forward-looking sonar data appears in Figure 4. This view shows the clumped test field. The four bright spots to the right of center are returns from targets around the outer ring.

The electro-optic, laser scanning sensor sweeps a blue-green beam across a 70 degree swath of the seafloor directly below the sensor. Images of the bottom from the sensor have a resolution of better than one cm. A blue-green laser was chosen because it has good range in water while still being in the visible spectrum. The range of the sensor is over five times that of a normal underwater camera. The sensor was used in a snapshot mode during the Feasibility Demonstration. An operator directed the sensor to record snapshot images when interesting objects were visible. An example of the electro-optic sensor data appears in Figure 5. The electro-optic sensor covers a narrow swath beneath the depressor and the displayed image shows only a small portion of the center region of the clumped test field.



Figure 5 - Electro-optic Sensor Image of Resolution Panels in Clumped Field

### Sensor Processing

The MUDSS system uses a Global Positioning System (GPS) receiver to determine the boat's position during a survey run. The GPS data is recorded in a computer file for later analysis. Boat position and heading are recorded, along with a timestamp, approximately once every second. Differential mode is used, which determines the position relative to a known point on shore, to reduce the error in unaided GPS data. The data in the individual sensor bands is timestamped also and the timestamps can be matched to the GPS file to determine boat position when a particular data item was being captured. The geometry of the system is known such that the positions of the depressor and towfish can be determined from the boat position and heading.

Due to the effectiveness of the low frequency side-looking sonar, it serves as the baseline sensor for the MUDSS system. Once beamforming has been performed on the sonar data, an orthorectification step transforms the range-based data into an orthonormal projection, i.e. a top-down view. Figure 6 illustrates the process. An estimate of the depth of the water column below the sensor is made from the low frequency sonar image which is used to map the range bin data onto a plane. At this stage of the process, the seafloor is assumed to

be perfectly flat and level as insufficient information is available to determine crosstrack slope or topography.



Figure 6 - Ortho-rectification Process

Next, Automatic Target Recognition Processing (ATRP) algorithms process the data to determine a set of likely targets. For the low frequency sonar data, the ATRP applies a Holmes single-gated filter (a double-gated is more robust but computationally more intensive and not necessary for these relatively uniform images), followed by a clutter filter, a size sieving algorithm, and an adaptive peak detection algorithm. The high-frequency sonar data is processed with a clutter reduction filter, followed by a linear wavelet transform and a peak detection algorithm. These algorithms produce a set of potential targets detected within the sonar image. This set of targets is originally represented in terms of (x,y) pixels from the corner of the image. Using GPS data and timestamps for the scanlines of the image, the track of the sensor can be determined and the pixel coordinates converted to Universal Transverse Mercator (UTM) or GPS coordinates. The set of potential targets is then recorded into a database to be registered with potential targets detected within other sensor bands or during other runs.

Figure 7 illustrates the results of the ATRP algorithms processing an orthorectified image. The suspected target positions are designated by boxes. The positions, in pixels and UTM coordinates, of a selected set of suspected targets are given in Table 1, along with the known positions of the test ordnance from the original placement. The ordnance positions are specified as Easting and Northing, in meters. Note that at this stage echoes from multipathing cannot be distinguished from actual target returns with certainty, only a high probability. However, only actual targets with known positions are included in the table.

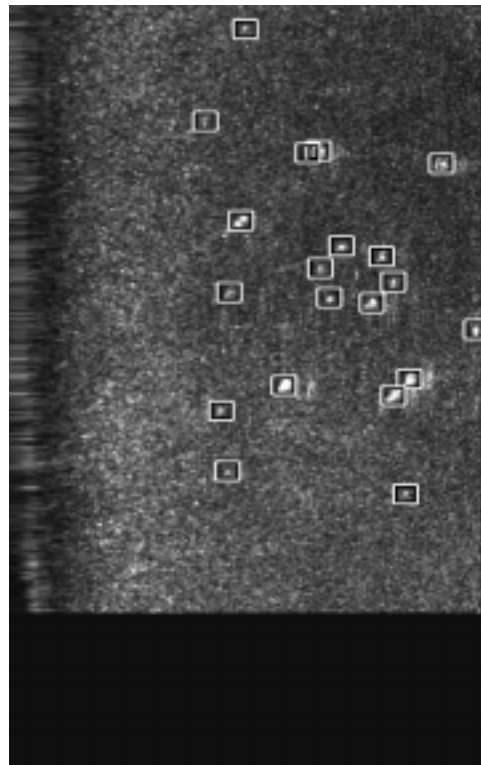


Figure 7 - Targets Detected in Low Freq. Data

Comparing the computed positions of the targets to the known positions shows a large discrepancy. Analysis of the alongtrack error for this set of targets shows a discrepancy of approximately 61 meters. This error is much larger than would be expected due to differential GPS error and is almost certainly due to erroneous timestamps. Analysis of the crosstrack error, which should be due solely to GPS error, shows a discrepancy of 2 meters, a very reasonable number. Table 2 lists the crosstrack and alongtrack error for a set of runs. Notice that runs 2, 6, and 7 in the table have alongtrack errors in the same range as the cross track errors while runs 1, 3, 4, and 5 have very large alongtrack errors. The large, inconsistent errors in alongtrack position, combined with the small, consistent errors in crosstrack position, indicate a definite problem with timestamps. However, the data serves to characterize the GPS error to be on the order of 5 meters or less.

Pixel X	Pixel Y	Computed E	Computed N	Known E	Known N
291	365	625845.8	3334537.5	625890.6	3334495.3
324	149	625858.5	3334519.8	625899.8	3334478.2
170	206	625866.1	3334535.4	625906.6	3334493.5
279	238	625855.7	3334529.5	625900.4	3334487.0

Table 1 - Location of Selected Targets from Low Frequency Sonar

Run	Alongtrack Error (meters)	Crosstrack Error (meters)
1	61.0	2.0
2	1.3	4.0
3	12.4	1.8
4	17.6	1.4
5	49.9	4.5
6	0.1	1.0
7	5.2	0.6

Table 2 - GPS Location Error Values

In a similar manner, the high frequency side-looking sonar data is orthorectified, using the water column depth from processing the low frequency data, and the ATRP algorithms are used to locate potential targets. Figure 8 shows the locations of the suspected targets identified by the ATRP algorithms. The low number of detections and the relatively high number of false detections indicates that the algorithms are not as robust for this type of data. Iterative techniques, using a fusion of data from other sensor bands, are expected to help this problem. These techniques are discussed in the Data Fusion section.

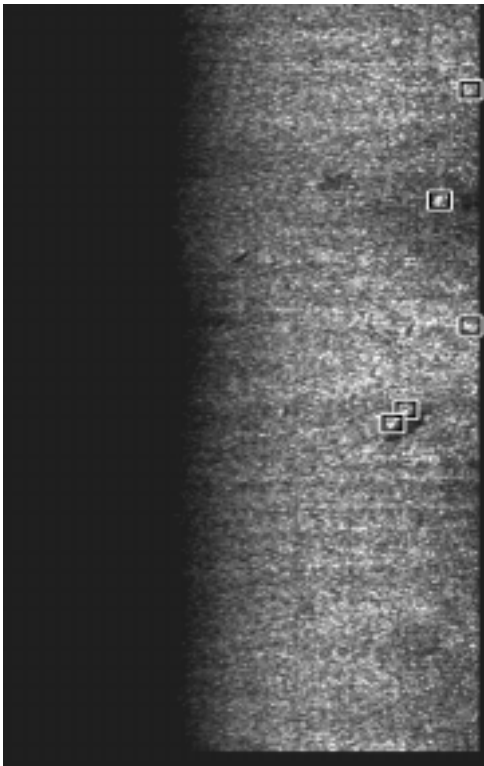


Figure 8 - Targets Detected in High Freq. Data

The superconducting magnetic field gradiometer detects ferrous objects based on their effect on the earth's magnetic field. The gradiometer collects a set of moments and

gradients at a 20 Hz rate in a file with timestamps. The file of moments and gradients is postprocessed to determine a set of magnetic dipoles which will produce the input data. The solution is not exact and there is a limit of six targets which may be distinguished within a 50 meter section of data. Thus the clumped field targets cannot be resolved since there are 12 targets in the two concentric rings. A number of false detections often occur in the gradiometer results. These may be detected by the confidence value and the position, since ordnance will generally be on or below the seafloor.

There are a total of 15 known targets in the linear test field, two sonar only and 13 magnetic. The gradiometer initially detected a total of 44 targets during the sample run providing this data. Of the 13 expected targets, 12 were in the list of 44 with a large number of false detections. Analysis of the gradiometer data alone allows many of the false targets to be rejected. First, the targets which are at inappropriate depths are eliminated. In this case, limiting the depth to a range of 3.5 to 6 meters culls the target list to 21 possibles while eliminating no known targets. The second culling removes duplicated targets. The gradiometer algorithms process the data in overlapping sections and the same target may be detected twice in the overlapped area. This trims the list to 18 and also does not remove any known targets. The final step removes targets with a low confidence value. In this case, a limit of 0.2 was chosen which reduced the list to 14 suspected targets but eliminated one known target. Thus, of the 14 remaining suspected targets, 11 were known and 3 were false detections. Table 3 lists the GPS position of the 14 suspected targets, along with the GPS position of the known target associated with the detection. Targets 1, 2, and 10 do not correspond to known targets. The confidence values of targets 1 and 2 are relatively low and are comparable to the lowest confidence values for the known targets. The confidence value for target 10 is relatively high and is likely unknown debris.

Table 4 lists the type of ordnance placed at the 15 locations in the linear field, along with the magnitude of the magnetic moment, the computed distance to the target, and a notation as to whether the ordnance was detected by the gradiometer. Note that the two missed targets were the largest and were expected to be detected. However, they were located 20 meters beyond the other targets along the line and may have been outside the gradiometer's range. Performance estimates for the gradiometer are based on manufacturer specifications so the expected range may not be accurate. Also, the linear field was laid out in such a way as to test the resolution of the gradiometer. It might locate the two missing targets if the field were slightly less dense. The two icosahedrons are aluminum sonar targets and should not be detected by the gradiometer.

Target	Easting	Northing	Confidence	Known East	Known North
1	626099.8	3334306.8	0.25	n/a	n/a
2	626099.6	3334289.3	0.47	n/a	n/a
3	626099.3	3334224.8	0.89	626098.4	3334224.8
4	626099.3	3334208.9	0.83	626098.3	3334210.5
5	626099.2	3334187.3	0.65	626098.1	3334188.4
6	626107.4	3334171.6	0.80	626107.7	3334170.5
7	626097.1	3334162.1	1.66	626098.2	3334160.8
8	626098.9	3334122.1	0.66	626099.6	3334122.9
9	626109.6	3334109.8	0.84	626107.8	3334106.8
10	626102.2	3334084.4	1.36	n/a	n/a
11	626092.2	3334074.3	0.29	626099.3	3334084.3
12	626099.5	3334051.2	2.12	626098.9	3334051.0
13	626112.3	3334047.2	0.26	626108.8	3334046.6
14	626098.9	3334030.3	0.45	626099.1	3334027.6

Table 3 - Suspected Targets Located by Gradiometer

The snapshot images from the electro-optic sensor are timestamped and the sensor position when the snapshot was captured can be determined. The timestamp of the snapshot shown in Figure 5 is 08:34:56, September 21, 1995. Referring to the GPS data for this run, the expected position for the electro-optic sensor is (625896.2, 3334466.8) in UTM coordinates. Given that the image in the electro-optic snapshot shows the center of the clumped field, the sensor position should be about four meters north of the center which is known to be at (625900.4, 3334490.0). The position determined from the GPS file shows about a four meter error in the crosstrack (easting) direction and about a 31 meter error in the alongtrack (northing) direction. It is likely that there is timestamp error in this data as well. Registration of the snapshots to the data from the other sensor bands is discussed in the Data Fusion section.

The forward-looking sonar produces a video stream of images with clock information within the video frame. The

Ordnance Type	Magnetic Moment	Distance (meters)	Detect
Icosahedron	0.0	5	N
60 mm mortar shell	515	4.5	Y
60 mm mortar shell	955	4.6	Y
105 mm mortar shell	1756	4.5	Y
55 gal drum	40752	9.1	Y
175 mm howitzer shell	17182	5.0	Y
MK84 2000-lb bomb		23	N
203 mm howitzer shell	8705	4.0	Y
55 gal drum	81123	11.0	Y
106 mm howitzer shell	2789	8.3	Y
MK83 1000-lb bomb		23	N
105 mm howitzer shell	2498	3.7	Y
MK82 500-lb bomb	68646	13.8	Y
60 mm mortar shell	110	3.6	Y
Icosahedron	0.0	4	N

Table 4 - Gradiometer Characteristics of Known Targets

sonar was used to collect data during the Feasibility Demonstration but the data has not been analyzed to date. It is planned to capture video frames at a rate of 1 or 2 Hz and process them through an ATRP algorithm to track targets. The sonar also has a digital output channel, currently unused, the use of which is discussed in the Future Work section.

### Data Fusion

Data fusion is the process of taking information from multiple, independent sensor bands and combining it to extract information not available in a single band. This process includes determining spatial relationships

between data sets from various sensor bands and multiple passes, identification of ordnance from multisensor data, and extracting topographic models of the seafloor.

Since the data from the MUDSS system is inherently spatial, the spatial relationships between the bands must be determined. In addition, multiple passes over the same area from different aspects provides additional sensor data to be fused. GPS data provides the basic tool to spatially register the various sensor data. The individual ATRP algorithms will process each sensor band and produce a list of suspected targets in each band. Since targets are expected to show up in multiple bands, the positions of the targets in each band may be used to further register the bands, improving upon the accuracy of the GPS data. Figure 9 shows an orthorectified view of the linear target field using the low frequency side-looking sonar. Overlaid on it are circles indicating the computed positions of the suspected targets detected by the magnetic field gradiometer. The circles have been mapped to their locations from their original gradiometer relative positions using GPS data alone. Note that the target positions detected by the gradiometer have the same shape and relative position as the bright spots indicating targets in the sonar data. The positions are displaced somewhat as a function of GPS error, with some error in the system geometry measurements. Measurement of the displacement may be used to refine the target positions to improve upon the GPS positioning.

Targets detected within each sensor band are recorded in a central target database. The database may be queried by the ATRP algorithms as to the expected location of a target in another band. As mentioned previously, the current ATRP algorithms are not as effective processing the high frequency sonar data. A potential technique, which has yet to be fully explored, for improving the algorithms in this area is the use of bounded techniques. The algorithms are necessarily not as robust when required to process an entire sonar image. False targets are nearly as prevalent as real ones. By using the target database to provide a list of expected target locations in the high frequency band, the ATRP algorithms can



Figure 9

concentrate their processing on those specific areas and detect only those targets within the bounded areas. The boundary will be large enough to allow for GPS errors and for probability measures for the other sensors. The targets found by the bounded algorithms will be added to the database. The target database contains position and confidence values and other sensor specific values which are used to coalesce the disparate lists into a single target list for the survey area. Multipathing echoes can be distinguished from

actual target returns using the target database and correlation techniques. Targets found along a horizontal line from a suspected target can be annotated as a potential echo by the ATRP algorithms to aid in this process. Actual targets will have a strong correlation between different passes and will register to the same location. Echoes will not correlate and can thus be recognized and removed from the target list.

Another aspect of data fusion is the classification and identification of the targets as specific ordnance. Each type of ordnance will have a specific signature in each band, depending upon aspect, how deep it is buried, and other factors. The key signatures are the size and material type, which dictate the sonar signal return strength, and the ferrous mass, which dictates the gradiometer results. Figure 10 illustrates how these signals can be used to distinguish ordnance from clutter in a survey area. Targets detected with the appropriate characteristics may be revisited with the electro-optic sensor to image the ordnance for specific identification. Figure 9 showed the gradiometer detected target positions overlaid on sonar data. Note the correlation between sonar return and the magnetic moments listed in Table 4. The larger targets tend to have a brighter sonar return. The ATRP algorithms can be made more robust, with better false detection rejection, by comparing a target's signature in multiple sensor bands.

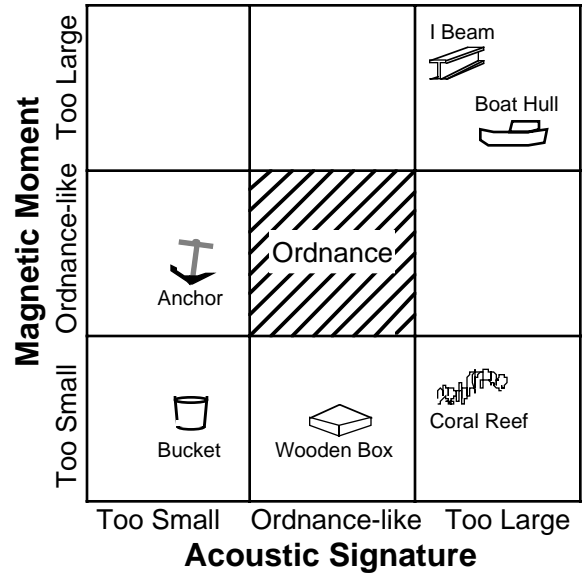


Figure 10 - Acoustic and Magnetic Data Fusion

The third aspect of data fusion is the production of three-dimensional topographic models of the seafloor from multiple passes of the various sensors over a survey area. This process is discussed in more detail in the Data Visualization section.

### Data Visualization

There are two primary types of data visualization used within the MUDSS system. The first is a two-dimensional display and replay of the sensor data for operator review. Several software tools have been developed for this purpose. The second is a three-dimensional flythrough capability for reviewing the topography of the seafloor in preparation for remediation activities. Some software tools have been developed for this purpose and some remain under development.

Two-dimensional replay serves a variety of purposes within the MUDSS system. The first use is a real-time review of sensor coverage within a survey area. It is important to be able to ensure that the appropriate sensors have surveyed the majority of the survey area. An example of the output of the Site Survey Tool (SST) appears in Figure 11. The SST provides real-time feedback on the instantaneous coverage and coverage history of each sensor in the suite. Instruments, such as the gradiometer, which have different effective ranges for different types of ordnance can be shown with varying coverage areas.

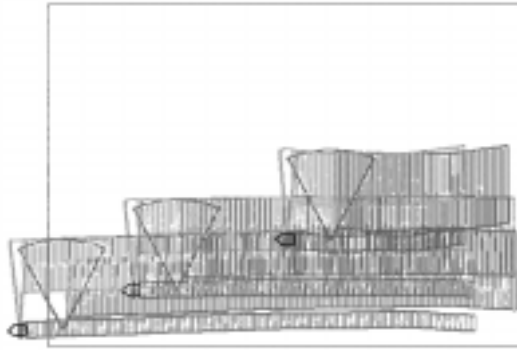


Figure 11 - Display of Coverage Area for Side-Looking Sonars and Electro-optic Sensor

Typically, the majority, if not the entirety, of the survey area is mapped with the side-looking sonars and the gradiometer. Effective search patterns may be devised and followed using the SST and coverage reviewed in realtime. Suspected targets may be revisited using the forward-looking sonar and GPS and imaged with the electro-optic sensor.

The other two-dimensional data visualization technique is reviewing individual sensor bands and the spatial relationships between different bands to augment the ATRP algorithms with operator review. An example of electro-optic data overlaid on sonar data appears in Figure 12. The operator can view the data covering a suspected target and annotate the target database.

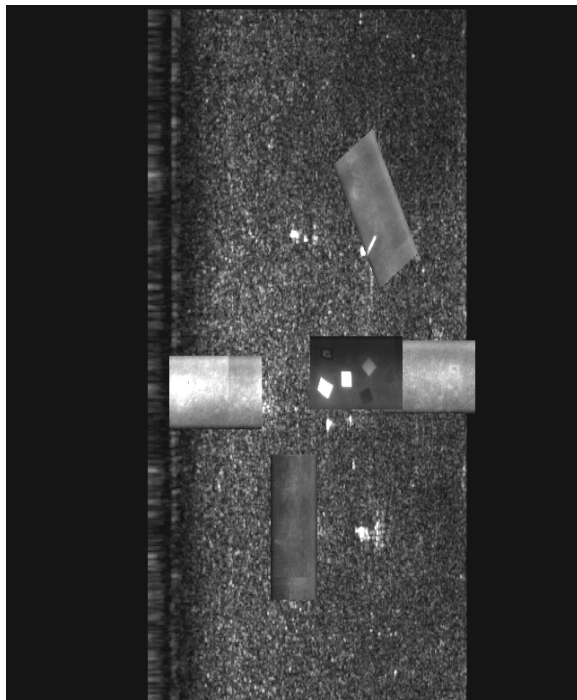


Figure 12 - Electro-optic Sensor Data Overlaid on Sonar Data

Three-dimensional data flythroughs are of value in areas where the seafloor is more rugged or contoured. In particular, part of planning a remediation activity is determining the slope and other topographic characteristics around an ordnance to be removed. Several sensors provide information which can be used to generate a three-dimensional model of the seafloor. The initial data source is the low frequency sonar. Since this sonar gets a bottom return directly below the sensor, a bottom profile along the sensor track can be extracted. This process would be aided tremendously by the addition of a fathometer to the sensor suite. The bottom profiles are combined into a single data set with all profiles normalized to remove differences due to tidal changes or variations in the depth of the sensor. A contour filling program can then generate estimates of bottom height for the unsampled portions of the survey area.

The second step is comparison of orthorectified bottom images generated from different aspects. These images act as stereo pairs and elevation information can be extracted. However, the targets will need to be used to correlate the pairs as there is a significant amount of noise which is different from different aspects and cannot be used for correlation. This means that the elevation resolution of the multiple image correlation is low. In general, only slope and other gross features will be detectable and then only in areas with targets or other sources of strong returns. To augment this topography model, the high-frequency sonar data can be used to extract feature heights from the length of the shadows cast by those features.

Once the topography model has been generated, software tools have been developed to perform three-dimensional flythroughs of the data. Figure 13 shows an image generated with such a tool. Because the test area was very flat, the topography has been modified by raising the bottom as a function of sonar signal return strength. This view shows spikes in the pattern of the clumped test field.

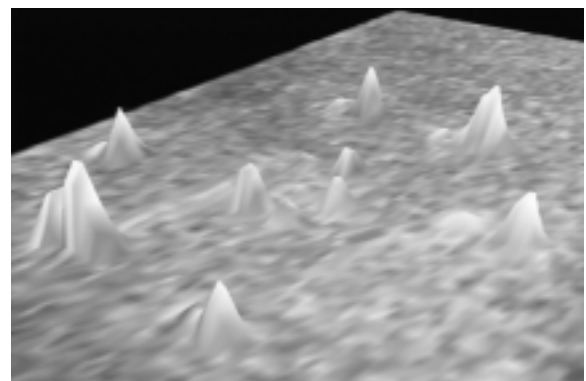


Figure 13 - 3D Visualization of Sonar Return for Clumped Target Field

### **Conclusions**

The MUDSS project has demonstrated the feasibility of using multiple sensors, with sophisticated multisensor fusion and visualization techniques, to locate ordnance on the seafloor. The low frequency side-looking sonar paired with the magnetic field gradiometer have been shown to effectively locate a variety of ordnance. The electro-optic sensor demonstrates excellent range and resolving power for making final identifications of suspected ordnance. GPS data provides a good starting point for registering the data from multiple sensors and crossmapping detected targets from one band to another. Multisensor data fusion provides the capability to more precisely locate ordnance and to distinguish ordnance which have similar characteristics. Data visualization provides the operator with the tools to direct an effective search and locate mission and to review data for remediation planning. Many of these issues are of value to AUV operations. However, this is ongoing work and several research issues remain which are discussed in the Future Work section.

### **Future Work**

Analysis of the Feasibility Demonstration data is not yet complete and several efforts remain. In particular, discrepancies in timestamps will be resolved such that GPS data can be used to determine the relative positions of all the sensor data with good accuracy. New ATRP algorithms for the high frequency sonar data and for the bounded techniques will be developed. Also, the forward-looking sonar has been little used to date. Capturing the video and analyzing it for targets will be done in the near future.

Once the Feasibility Demonstration data has been thoroughly analyzed, Phase II of the project will commence. This second phase, the Technology Demonstration, will see changes in both hardware and software. In the hardware, the sensors will be combined into a single housing, along with a fathometer, a doppler sensor, and a chemical sensor. Meanwhile, the software and computing systems will be integrated into a cohesive system with synchronized timestamps, target databases accessible throughout the system, and on the fly visualization of data. Real-time access to all data streams will be available. Use of the digital data stream from the forward-looking sonar will enhance its usefulness for detecting ordnance. The sonar has a built-in target detection capability and a list of detected targets is output regularly over the digital channel. This target list will augment the ATRP algorithms and provide additional sensor data to fuse. In addition, real-time analysis of the sonar data will provide reacquisition capability to allow the operator to direct the sensors to pass directly over a suspected ordnance. This will be useful for allowing the electro-optic sensor to get the best view of the ordnance. In the case of buried targets, the chemical sensor will be used to take sediment samples directly over the target for analysis to detect explosives. The presence of explosives will indicate ordnance and the type of explosive can be used to identify the particular type of ordnance. This Technology Demonstration system will be fielded as an integrated unit, available for use in any shallow water environment.

### **Acknowledgments**

The work described in this paper was performed at the Jet Propulsion Laboratory, California Institute of Technology, under a contract with the National Aeronautics and Space Administration.